Projectile angular-differential cross sections for electron transfer processes in ion-helium collisions: Evidence for the applicability of the independent electron model

Myroslav Zapukhlyak*
Max Planck Institute for the Physics of Complex Systems, D-01187 Dresden, Germany

Tom Kirchner†
Department of Physics and Astronomy, York University, Toronto, Ontario, Canada M3J 1P3
(Received 11 September 2009; published 3 December 2009)

The electron dynamics in p-He and He^{2+}-He collisions have been investigated on the level of the independent electron model by using the two-center basis generator method. Projectile angular-differential cross sections for various one- and two-electron processes involving electron transfer have been calculated with the eikonal approximation. Overall, the calculated cross sections are in good agreement with the most recent experimental cold target recoil ion momentum spectroscopy data taken at impact energies in the range from 40 to 630 keV/amu. This demonstrates, somewhat surprisingly, that electron correlations play but a minor role for the processes and the energies considered.

DOI: 10.1103/PhysRevA.80.062705 PACS number(s): 34.50.Fa, 34.70.+e

I. INTRODUCTION

Ion-atom collisions and in particular electron transfer processes have been investigated intensely over many years. Not only is this research motivated by the quest for a better understanding of the fundamental few-body dynamics, but it has also practical implications for applied fields, such as plasma physics and fusion research.

For a long time, theoretical and experimental efforts concentrated on the energy dependence of total cross sections (TCSs). More recently, accurate fully differential cross section (DCS) measurements have become feasible thanks to the development of cold target recoil ion momentum spectroscopy (COLTRIMS) [1–4]. COLTRIMS has brought a turning point for the theoretical description of collision processes since it enables tests of theories and comparisons between different models on a much more detailed level.

Ion-helium collisions are prime candidates for such investigations. A recurring theme in numerous studies of these systems has been the question of how strongly electron-correlation effects might influence the collision dynamics and, in turn, where exactly the limits of the independent electron model (IEM) are situated. Recent studies have also demonstrated that the role of the nucleus-nucleus interaction is less well understood than one might have thought [5–8].

Motivated by recent COLTRIMS data [9] and theoretical works [10–14] we attempt to clarify the problem by exhausting the framework imposed by the semiclassical approximation (SCA) and the IEM. We have concentrated our efforts on striving for well-converged and numerically stable solutions of the ensuing set of equations in order to obtain results that shed light on the validity of the framework itself. We consider situations in which the projectile deflection angle and the final states of the electrons are determined, i.e., we calculate fully differential cross sections and compare them to measurements for proton and He^{2+} impact. As it turns out, a number of one- and two-electron processes involving electron transfer and excitation can be described quite well. This does not mean that electron correlations are absent in these collision systems, but it signals that their effects are rather small at intermediate impact energies for quite a few cases.

II. THEORY

The theoretical description we are using is the same as in Ref. [7]. Therefore, we only give a brief summary here. As mentioned above, our treatment is based on the SCA and the IEM, i.e., the electrons are driven by classically moving nuclei, and the Hamiltonian is assumed to be of single-particle form with an effective ground-state potential that models the electron-electron interaction. The time-dependent single-particle Schrödinger equation is solved with the two-center basis generator method (TC-BGM), which is a nonperturbative coupled-channel method that includes dynamically adapted basis states [15,16]. The electronic many-particle transition amplitudes are then reconstructed consistently in the IEM picture and transformed from impact-parameter- to momentum-transfer-dependent quantities by using the well-known eikonal approximation [17–19].

It is clear that the approximations in each of these steps can play a role and impair the resulting DCSs. Nevertheless, by exercising special care with the computational implementation and basis set convergence, the IEM and the eikonal approximation themselves are tested. No other restrictions, such as perturbative arguments are involved.

For a few one- and two-electron processes theoretical calculations based on continuum distorted-wave-like methods were reported previously. The detailed comparison of our DCS with those and with recent COLTRIMS data provides points of reference, where the limitations of the theoretical descriptions are located.

III. RESULTS AND DISCUSSION

As already mentioned, the main motivation for this work is the availability of detailed COLTRIMS data for p-He and

*zmi@pks.mpg.de
†tomk@yorku.ca

TABLE I. Q values for relevant final states and used abbreviations for different one- and two-electron processes in p-He and He^{2+}-He collisions [9].

p-He				He^{2+}-He			
Abbrev.	Final state	Note	Q value (a.u.)	Abbrev.	Final state	Note	Q value (a.u.)
SC1	$H(1s)+He^+(1s)$		−0.4	SC1	$He_P^+(1s)+He_T^+(1s)$		1.1
SC2	$H(nl)+He^+(1s)$	$n\geq 2$	−0.78	SC2	$He_P^+(nl)+He_T^+(1s)$	$n=2$	−0.4
SC3	$H(1s)+He^+(nl)$	$n\geq 2$	−1.9		$He_P^+(1s)+He_T^+(nl)$		
SC4	$H(nl)+He^+(nl)$	$n\geq 2$	−2.28	SC3	$He_P^+(nl)+He_T^+(1s)$	$n\geq 3$	−0.68
					$He_P^+(1s)+He_T^+(nl)$		
				SC4	$He_P^+(nl)+He_T^+(nl)$	$n\geq 2$	−1.9
				DC1	$He_P(1s^2)+He_T^{2+}$		0.0
				DC2	$He_P^+(1s,nl)+He_T^{2+}$	$n\geq 2$	−0.73

He^{2+}-He collisions [9]. So far, comparisons to calculations have only been conducted for some of these measurements [7,14]. We are using the nomenclature of Ref. [9] (see Table I). Only reactions in which (at least) one electron is transferred to the ground state or to an excited state of the projectile are considered. The other electron is either known to remain in the target ground state or it is excited or also captured (in the case of He^{2+} projectiles). We are not concerned with free electrons in this work.

The different reaction channels can be distinguished by their Q values, i.e., the differences between the total (negative) binding energies of the electrons before and after the collision. For small scattering angles and small energy transfer Q can be identified with the change in the kinetic energy of the projectile, which means that it is nothing else than the inelasticity of the collision [20]. Experimentally, the Q value is determined via measuring the momentum component of the recoiling target ion along the projectile beam axis. The somewhat unusual separation of processes in Table I corresponds to the resolution of the COLTRIMS experiment [21].

In Refs. [9,14] only relative DCSs were measured. They were normalized to the experimental absolute TCSs shown in Figs. 1 and 2 by appropriate integration over the scattering angle. In the theoretical calculations we obtain absolute state-to-state DCS, where according to the IEM the final two-electron states are given as (symmetrized) products of single-particle states. In order to compare these results to the measurements all individual cross sections which correspond to a channel that could be resolved experimentally have been summed up.

A. Total cross sections

We begin the discussion of results with the TCS for single capture (SC) and double capture (DC) in He^{2+}-He collisions (Figs. 1 and 2). Single capture can take place either as a pure one-electron process or together with target excitation. We will refer to the latter process as transfer excitation (TE). The TCS for single capture in the p-He collision system was already published in our previous work [7]. There, very good agreement with measurements was found from 2 keV up to 2 MeV impact energy.

The He^{2+}-He collision system is a resonant two-electron system with the remarkable property that two-electron capture is stronger than single capture at low impact energies E_P. Only at $E_P\approx 15$ keV/amu is the predominance of one-electron capture re-established. This behavior was reproduced by two-electron calculations which included electron-correlation effects [31–33], but not by the IEM, even if time-dependent screening and exchange was included appropriately [34].

For the sake of conciseness, those previous theoretical results are not included in Figs. 1 and 2. Rather, only the present TC-BGM calculations are compared to experimental data. Above $E_P\approx 20$ keV/amu the agreement is good for both single and double captures. This implies that even two-electron processes can be described on the level of the IEM in this region, and it appears worthwhile to investigate whether this is also true for *differential* cross sections. This is the topic of Secs. III B and III C.

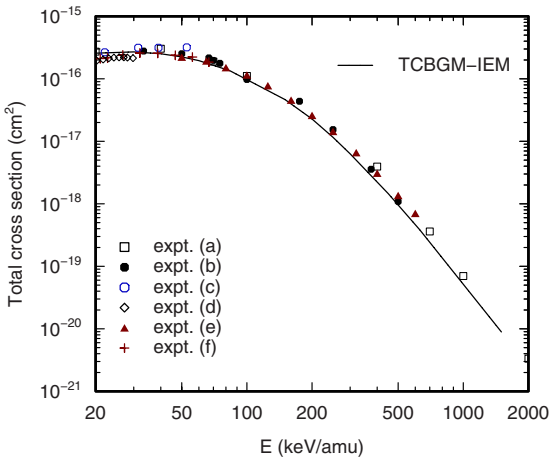

FIG. 1. (Color online) Total single transfer cross section as a function of impact energy for He^{2+}-He collisions. Theory: present TC-BGM calculation within IEM; experiment: (a) [22], (b) [23,24], (c) [25], (d) [26], (e) [27], and (f) [28].

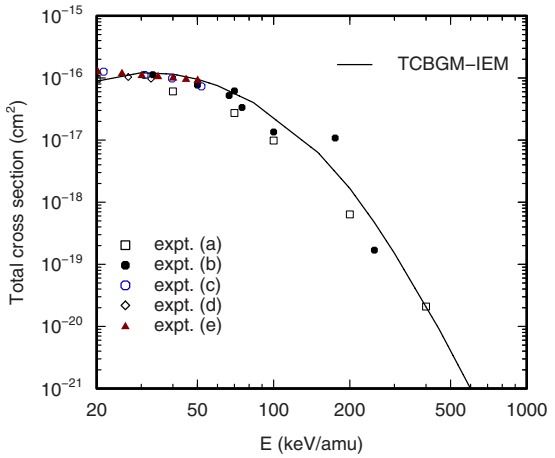

FIG. 2. (Color online) Total double-electron transfer cross section as a function of impact energy for He^{2+}-He collisions. Theory: present TC-BGM calculation within IEM; experiment: (a) [22], (b) [23,24], (c) [25], (d) [26,29], and (e) [30].

B. Differential cross sections for single-electron transfer and transfer excitation

We first consider the p-He collision system. The data shown in Figs. 3 and 4 complement previous results at different impact energies which were presented in Ref. [7].

The DCSs for single capture into $n=1$ (SC1) and into $n \geq 2$ (SC2) are in good agreement with the measurements, in particular at small scattering angles (Fig. 3). In the case of SC1 we also compare our results to the continuum distorted-wave Born final state (CDW-BFS) calculations reported in Ref. [14]. At $E_P=150$ and 300 keV they exhibit peaks, which are reminiscent of the Thomas process. This is an interatomic double scattering process, which is, however, not expected to play a role at these impact energies. Furthermore, the CDW-BFS peaks are neither supported by the measurements nor by our results. On the contrary, the latter show quite distinct interference structures in this region. As explained previously, these are caused by an interplay of different terms in the eikonal integral, which are associated with projectile-electron and projectile-target-nucleus interactions [7,35].

At lower energies ($E_P=60-100$ keV), an oscillatory behavior of the DCS at relatively large scattering angles is indicated in the data for both SC1 and SC2 processes. One might speculate that they are due to an interference between different reaction pathways or an interference of amplitudes associated with separated coupling regions in the incoming and outgoing paths of the collision [9]. It cannot be expected that such oscillations are completely reproduced by our theoretical model since it employs a common eikonal phase for all transitions. This might average and smear out phase-sensitive information. As a matter of fact, oscillations are absent in our calculated DCS.

A similar comment applies to Fig. 4, which displays results for two TE channels that could be distinguished in the experiment: in SC3 one electron is transferred to the projectile ground state, while it ends up in an excited state in SC4 (cf. Table I). In both cases the transfer process is accompanied by target excitation. Except for the oscillatory behavior at large scattering angles our theoretical results follow the measurements quite closely. Given that the calculations are based on the IEM we conclude that electron correlations do not play a prominent role for these two-electron processes.

DCSs for different single transfer processes in the He^{2+}-He collision system are shown in Figs. 5 and 6. Note that the impact energies are not the same in all panels and that the resolved processes and, correspondingly, the nomenclature are different from those used for p-He collisions (cf. Table I). The only exception is SC1, which always refers to a single-electron capture process into the projectile ground state associated with a passive second electron.

The SC1 DCS for He^{2+} impact (Fig. 5) shows a few interesting features. First, an interference structure similar to the case of p-He collisions is present in the data at low projectile energies and small scattering angles. It disappears with rising projectile energy, and the TC-BGM calculations reproduce this behavior quite precisely. By contrast, the continuum distorted-wave Born initial state (CDW-BIS) calcula-

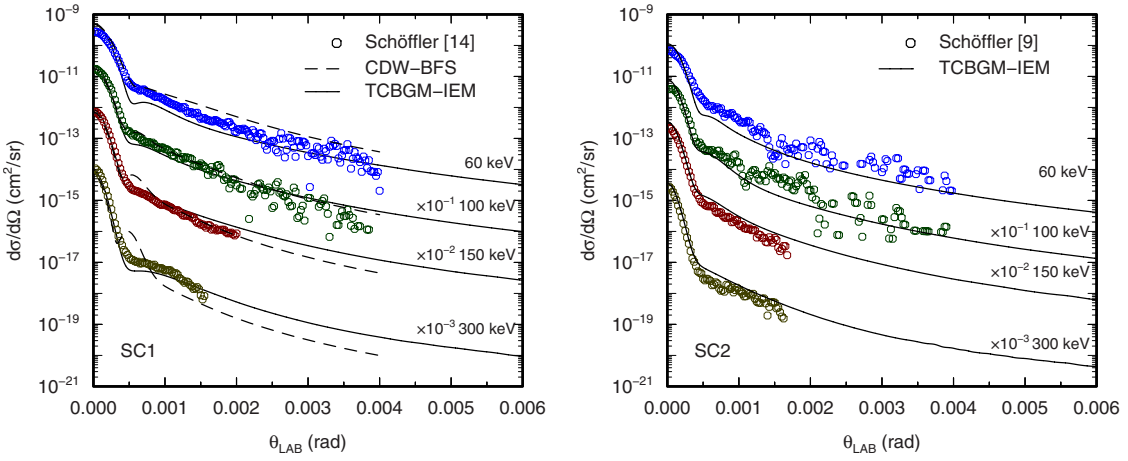

FIG. 3. (Color online) Differential single transfer cross sections as functions of laboratory scattering angle for $E_P=60-300$ keV p-He collisions. Theory: present TC-BGM calculations within IEM for single transfer into $n=1$ (left panel) and $n \geq 2$ (right panel) shells corresponding to SC1 and SC2 in Table I; CDW-BFS calculations for SC1 [14]. Experiment: Schöffler *et al.* [9,14].

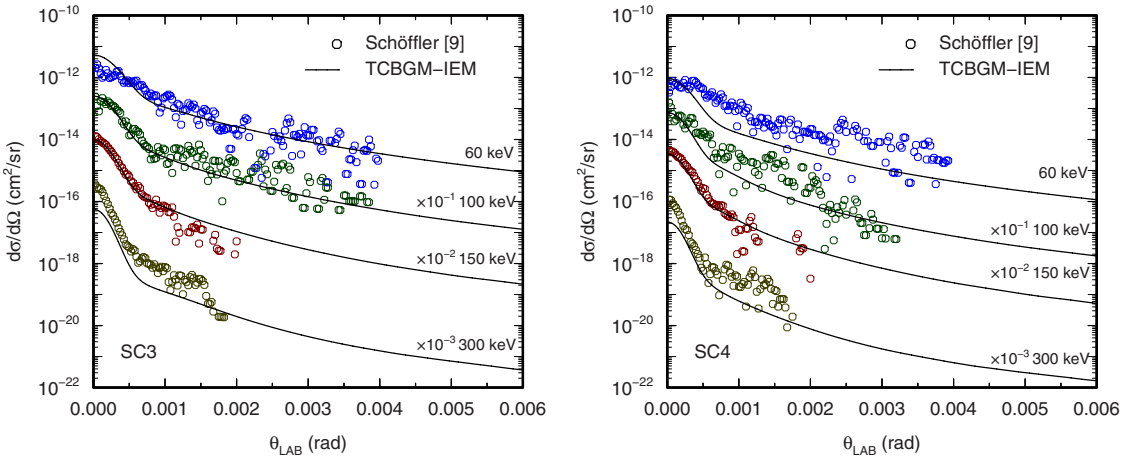

FIG. 4. (Color online) Differential transfer-excitation cross sections as functions of laboratory scattering angle for E_P=60–300 keV p-He collisions. Theory: present TC-BGM calculations within IEM for transfer-excitation processes corresponding to SC3 (left panel) and SC4 (right panel) in Table I. Experiment: Schöffler [9].

tions published along with the measurements exhibit pronounced dips in this angular region, which were blamed on a mutual cancellation of terms in the perturbation potential and considered unphysical [14]. Second, oscillations at larger scattering angles are again observable in the data in the energy range of E_P=40–60 keV/amu and are missing in the theoretical cross sections. The average of the experimental DCS is well reproduced.

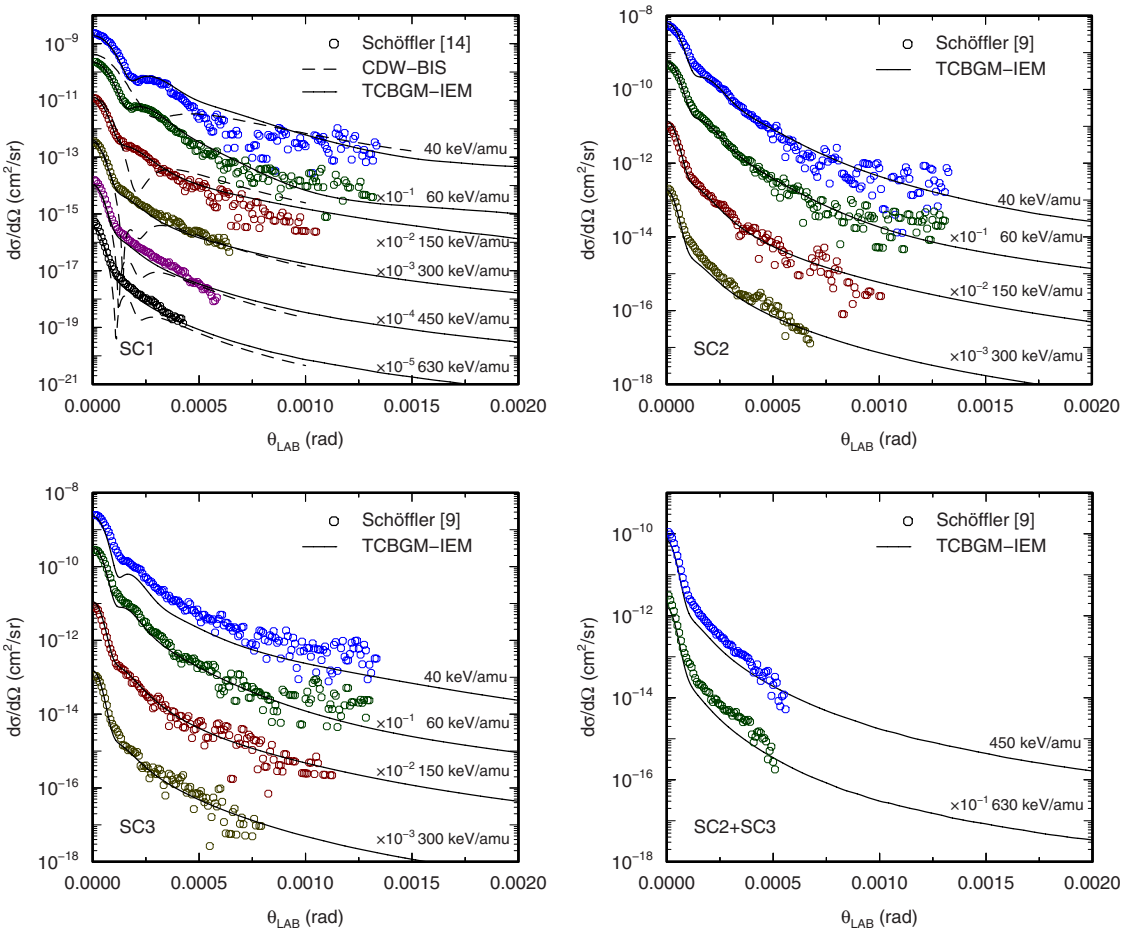

FIG. 5. (Color online) Differential single transfer and transfer-excitation cross sections as functions of laboratory scattering angle for E_P=40–630 keV/amu $^3He^{2+}$-^{4}He collisions. Theory: present TC-BGM calculations within IEM for processes corresponding to SC1 (top left), SC2 (top right), SC3 (bottom left), and SC2+SC3 (bottom right) in Table I; CDW-BIS calculations for SC1 [14]. Experiment: Schöffler *et al.* [9,14].

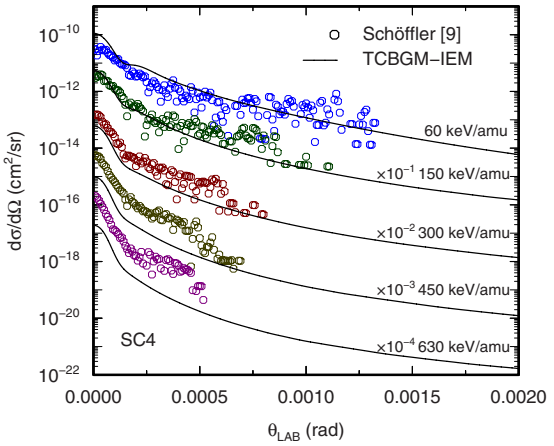

FIG. 6. (Color online) Differential transfer-excitation cross sections as functions of laboratory scattering angle for E_P=60–630 keV/amu $^3He^{2+}$-^4He collisions. Theory: present TC-BGM calculations within IEM for SC4 in Table I. Experiment: Schöffler [9].

These comparisons together with the data shown in Ref. [7] suggest that our theoretical model works better for He^{2+} than for proton impact. This is corroborated by the results for the SC2 and SC3 processes. These are sums of pure transfer and TE processes, which correspond to the same Q values. In the case of SC2, excellent agreement with the experimental data is achieved (Fig. 5). For SC3, the agreement is also satisfactory. Only at E_P=40 keV/amu are the experimental DCSs somewhat larger than the theoretical ones.

At the higher energies E_P=450–630 keV/amu only the sum of SC2 and SC3 was resolved experimentally. Also in these cases are the data somewhat underestimated by the calculations except for larger scattering angles, where the experimental DCS drops off rapidly.

Finally, Fig. 6 displays results for SC4, in which both projectile and target are in excited states after the collision. The comparison between calculations and data shows the same trends as before, and overall one can say that single transfer processes in the He^{2+}-He system are described fairly well by our theory. This provides further evidence for the minor role of electron-correlation effects and the applicability of the IEM.

C. Differential cross sections for two-electron transfer

DCSs for two-electron transfer in He^{2+}-He collisions are presented in Fig. 7. Despite the IEM description the experimental DCSs for the DC1 process, in which the neutralized projectile is found in the ground state, are well reproduced by our calculations. The agreement with the data is even better than in the case of the Born distorted-wave (BDW) calculation reported in Ref. [14], in which correlated initial and final states were considered. This indicates, somewhat surprisingly, that even on the differential level double capture is essentially an uncorrelated process in this energy range. For the DC2 process we observe some discrepancies between our calculations and the experimental data, but nonetheless the overall agreement is good and the minor importance of electron-correlation effects confirmed.

Finally, in Fig. 8 two-electron capture into all shells is considered at the somewhat higher impact energy E_P=1500 keV=375 keV/amu. This DCS was measured some time ago and compared with CDW calculations [36,37]. It was observed that the theoretical results improved only slightly if correlation effects in the initial and final states were included in the model in terms of configuration interaction (CI). A notable effect of these static correlations on the TCS could not be proven with certainty.

In addition to those previous results Fig. 8 includes DCS computed in this work, where double captures into the ground state (n=1) and into all shells (Σn) have been considered. Furthermore, correlated perturbative calculations of Ref. [13] are shown. In the CI-type calculations only transitions between the ground states were computed and the possible effects of correlation on double capture into excited states were not addressed. These effects might be of some significance and might explain why our IEM results for the DC2 process differ somewhat from the experimental data at lower impact energies (cf. Fig. 7).

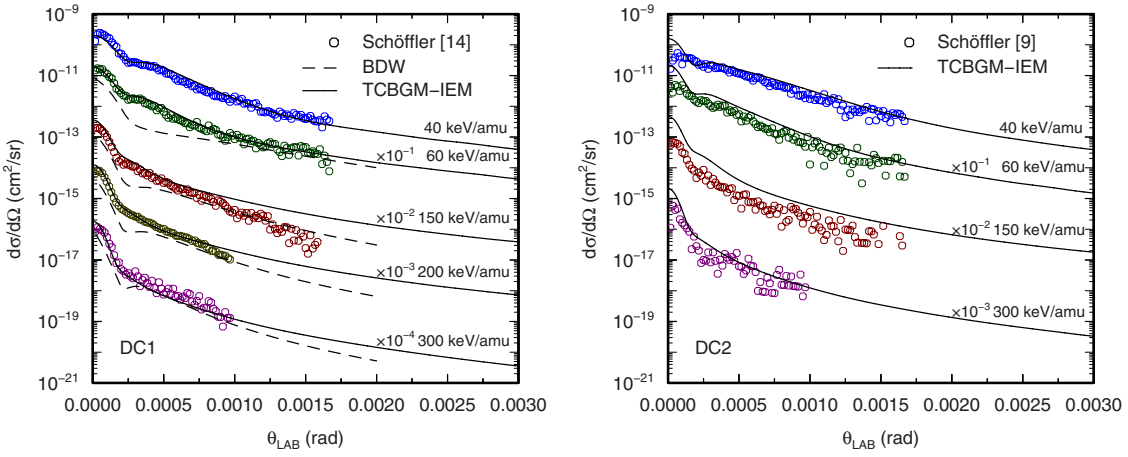

FIG. 7. (Color online) Differential two-electron transfer cross sections as functions of laboratory scattering angle for E_P=40–300 keV/amu $^3He^{2+}$-^4He collisions. Theory: present TC-BGM calculations within IEM for DC1 (left panel) and DC2 (right panel) in Table I; BDW calculations for DC1 [14]. Experiment: Schöffler *et al.* [9,14].

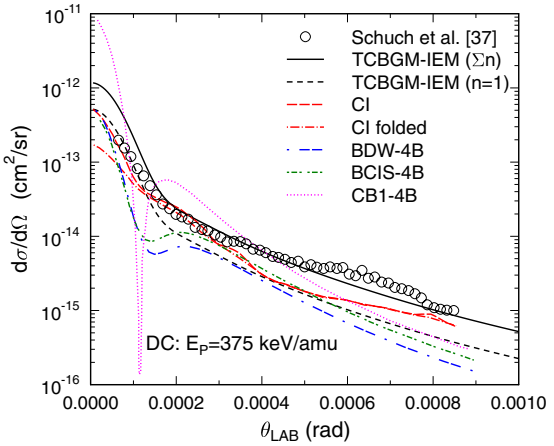

FIG. 8. (Color online) Differential two-electron transfer cross section as a function of laboratory scattering angle for E_P=375 keV/amu $^4He^{2+}$-^4He collisions. Theory: present TCBGM calculation within IEM for two-electron transfer into all shells (Σn) and into the ground state ($n=1$) of the projectile; CDW calculation with static correlation in the initial and final states (CI) [36,37]; same CDW calculation folded with the experimental resolution function (CI folded) [36,37]; four-body Born distorted wave (BDW-4B); boundary-corrected four-body first Born (BCIS-4B); four-body boundary-corrected continuum intermediate state (CB1-4B) calculations [13]. Experiment: two-electron transfer into all shells (Schuch *et al.* [37]).

However, according to our calculations there is no indication for correlation effects at the projectile energy E_P =375 keV/amu. Figure 8 shows that the IEM (Σn) calculation is in very good agreement with the measurements for scattering angles $\theta_{LAB} \geq 0.2$ mrad, but gives somewhat larger DCS at smaller angles. For the direct comparison with the measurements the CI calculation of Refs. [36,37] was folded with the experimental resolution function. The effect of this procedure can be seen clearly by comparing the DCS of the CI calculations (CI and CI folded): the convolution of the theoretical cross section with the experimental resolution reduces the cross section at small scattering angles, while the DCS at $\theta_{LAB} \geq 0.2$ mrad is unaffected. One can anticipate which consequences such a convolution will have on our IEM (Σn) DCS: excellent agreement with the experimental data might be achieved in the entire angular range. Unfortunately, the experimental resolution function was not available to us, so that we were not able to prove this conjecture.

IV. CONCLUSIONS

We have considered angular-differential cross sections for one- and two-electron processes in p-He and He^{2+}-He collisions in a rather broad range of impact energies. Our study clarifies some open points in the overall picture and provides important information for the further development of theories. Namely, the independent electron model which neglects electron-correlation effects does indeed provide an adequate framework to describe quite a few inelastic processes in these systems. Given that these effects were often thought to play an important role in *any* two-electron process, this is a remarkable and somewhat unexpected result.

A further important conclusion of our study concerns the quality and the nonperturbative nature of the single-electron transition amplitudes, which are used for the modeling of the two-electron amplitudes within the IEM. The details of our calculation show that high accuracy is crucial if the differential cross sections are computed with the eikonal approximation. Calculations based on perturbation theory and distorted-wave models sometimes exhibit unphysical structures and show in general less satisfactory agreement with the measurements, which might indicate the necessity to employ nonperturbative methods.

ACKNOWLEDGMENTS

We thank Markus Schöffler for fruitful discussions and for the communication of his experimental results in tabulated form.

[1] R. Moshammer, J. Ullrich, M. Unverzagt, W. Schmidt, P. Jardin, R. E. Olson, R. Mann, R. Dörner, V. Mergel, U. Buck, and H. Schmidt-Bocking, Phys. Rev. Lett. **73**, 3371 (1994).
[2] R. Dörner, V. Mergel, R. Ali, U. Buck, C. L. Cocke, K. Froschauer, O. Jagutzki, S. Lencinas, W. E. Meyerhof, S. Nüttgens, R. E. Olson, H. Schmidt-Bocking, L. Spielberger, K. Tokesi, J. Ullrich, M. Unverzagt, and W. Wu, Phys. Rev. Lett. **72**, 3166 (1994).
[3] J. Ullrich, R. Dörner, V. Mergel, O. Jagutzki, L. Spielberger, and H. Schmidt-Böcking, Comments At. Mol. Phys. **30**, 285 (1994).
[4] W. Wu, K. L. Wong, R. Ali, C. Y. Chen, C. L. Cocke, V. Frohne, J. P. Giese, M. Raphaelian, B. Walch, R. Dörner, V. Mergel, H. Schmidt-Böcking, and W. E. Meyerhof, Phys. Rev. Lett. **72**, 3170 (1994).
[5] M. Schulz, R. Moshammer, D. Fischer, H. Kollmus, D. H. Madison, S. Jones, and J. Ullrich, Nature (London) **422**, 48 (2003).
[6] N. V. Maydanyuk, A. Hasan, M. Foster, B. Tooke, E. Nanni, D. H. Madison, and M. Schulz, Phys. Rev. Lett. **94**, 243201 (2005).
[7] M. Zapukhlyak, T. Kirchner, A. Hasan, B. Tooke, and M. Schulz, Phys. Rev. A **77**, 012720 (2008).
[8] M. S. Schöffler, J. N. Titze, L. P. H. Schmidt, T. Jahnke, O. Jagutzki, H. Schmidt-Böcking, and R. Dörner, Phys. Rev. A **80**, 042702 (2009).
[9] M. Schöffler, Ph.D. thesis, Johann Wolfgang Goethe-Universität, Frankfurt am Main, 2006; http://publikationen.ub.uni-frankfurt.de/volltexte/2006/3536/
[10] I. Mančev, V. Mergel, and L. Schmidt, J. Phys. B **36**, 2733 (2003).
[11] P. N. Abufager, A. E. Martínez, R. D. Rivarola, and P. D. Fainstein, J. Phys. B **37**, 817 (2004).
[12] I. Mančev, EPL **69**, 200 (2005).

[13] D. Belkić, I. Mančev, and J. Hanssen, Rev. Mod. Phys. **80**, 249 (2008).
[14] M. S. Schöffler, J. Titze, L. P. H. Schmidt, T. Jahnke, N. Neumann, O. Jagutzki, H. Schmidt-Böcking, R. Dörner, and I. Mancev, Phys. Rev. A **79**, 064701 (2009).
[15] O. J. Kroneisen, H. J. Lüdde, T. Kirchner, and R. M. Dreizler, J. Phys. A **32**, 2141 (1999).
[16] M. Zapukhlyak, T. Kirchner, H. J. Lüdde, S. Knoop, R. Morgenstern, and R. Hoekstra, J. Phys. B **38**, 2353 (2005).
[17] R. J. Glauber, in *Lectures in Theoretical Physics*, edited by W. E. Brittin and L. G. Dunham (Interscience Publishers, New York, 1959), Vol. 1, pp. 315–414.
[18] L. Wilets and S. J. Wallace, Phys. Rev. **169**, 84 (1968).
[19] R. McCarroll and A. Salin, J. Phys. B **1**, 163 (1968).
[20] R. W. McCullough, F. G. Wilkie, and H. B. Gilbody, J. Phys. B **17**, 1373 (1984).
[21] Note in particular that the notations for p-He and He^{2+}-He collisions are different and SC2, SC3, and SC4 correspond to different channels and final states.
[22] *Atomic Data for Controlled Fusion Research*, edited by C. F. Barnett, J. A. Ray, E. Ricci, M. I. Wilker, E. W. McDaniel, E. W. Thomas, and H. B. Gilbody (National Laboratory, Oak Ridge, TN, 1990), Vol. 1; http://www-cfadc.phy.ornl.gov/redbooks/one/1.html
[23] R. D. DuBois, Phys. Rev. A **33**, 1595 (1986).
[24] R. D. DuBois, Phys. Rev. A **36**, 2585 (1987).
[25] K. H. Berkner, R. V. Pyle, J. W. Stearns, and J. C. Warren, Phys. Rev. **166**, 44 (1968).
[26] V. V. Afrosimov, A. A. Basalaev, G. A. Leiko, and M. N. Panov, Sov. Phys. JETP **47**, 837 (1978).
[27] M. B. Shah and H. B. Gilbody, J. Phys. B **18**, 899 (1985).
[28] M. B. Shah, P. McCallion, and H. B. Gilbody, J. Phys. B **22**, 3037 (1989).
[29] V. V. Afrosimov, G. A. Leiko, Y. A. Mamaev, and M. N. Panov, Sov. Phys. JETP **40**, 661 (1975).
[30] M. B. Shah and H. B. Gilbody, J. Phys. B **7**, 256 (1974).
[31] C. Harel and A. Salin, J. Phys. B **13**, 785 (1980).
[32] M. Kimura, J. Phys. B **21**, L19 (1988).
[33] K. Gramlich, N. Grün, and W. Scheid, J. Phys. B **22**, 2567 (1989).
[34] M. Keim, Ph.D. thesis, Johann Wolfgang Goethe-Universität, Frankfurt am Main, 2005; http://publikationen.ub.uni-frankfurt.de/volltexte/2005/1123/
[35] R. Gayet and A. Salin, Nucl. Instrum. Methods Phys. Res. B **56-57**, 82 (1991).
[36] G. Deco and N. Grün, Z. Phys. D: At., Mol. Clusters **18**, 339 (1991).
[37] R. Schuch, E. Justiniano, H. Vogt, G. Deco, and N. Grün, J. Phys. B **24**, L133 (1991).